J. Phys. B: At. Mol. Opt. Phys. **40** (2007) R39–R60 doi:10.1088/0953-4075/40/7/R01

TOPICAL REVIEW

The time-dependent close-coupling method for atomic and molecular collision processes

M S Pindzola[1], F Robicheaux[1], S D Loch[1], J C Berengut[1], T Topcu[1], J Colgan[2], M Foster[2], D C Griffin[3], C P Ballance[3], D R Schultz[4], T Minami[4], N R Badnell[5], M C Witthoeft[5], D R Plante[6], D M Mitnik[7], J A Ludlow[8] and U Kleiman[9]

[1] Department of Physics, Auburn University, Auburn, AL, USA
[2] Theoretical Division, Los Alamos National Laboratory, Los Alamos, NM, USA
[3] Department of Physics, Rollins College, Winter Park, FL, USA
[4] Physics Division, Oak Ridge National Laboratory, Oak Ridge, TN, USA
[5] Department of Physics, University of Strathclyde, Glasgow, UK
[6] Department of Mathematics, Stetson University, Deland, FL, USA
[7] Department of Physics, University of Buenos Aires, Buenos Aires, Argentina
[8] Department of Applied Mathematics, Queen's University, Belfast, UK
[9] Max Planck Institute for the Physics of Complex Systems, Dresden, Germany

Received 1 February 2007
Published 15 March 2007
Online at stacks.iop.org/JPhysB/40/R39

Abstract

We review the development of the time-dependent close-coupling method to study atomic and molecular few body dynamics. Applications include electron and photon collisions with atoms, molecules, and their ions.

(Some figures in this article are in colour only in the electronic version)

1. Introduction

The time-dependent close-coupling method was first applied to calculate total cross sections for the electron-impact single ionization of H [1, 2] and the photon-impact double ionization of He [3], which are the simplest quantal three-body Coulomb breakup problems. As pointed out by Bottcher [4], the time evolution of a wavepacket localized in space obviates the need for answers to questions about the asymptotic form of the wavefunction in position space or its singularities in momentum space. The time-dependent close-coupling method is a wavepacket solution of the same set of close-coupled partial differential equations used in the time-independent electron–atom scattering method of Wang and Callaway [5, 6].

In the last decade the original time-dependent close-coupling method on a 2D numerical lattice has been applied to calculate total and differential cross sections for electron-impact single ionization and photon-impact double ionization of many atomic systems. Recently, the time-dependent close-coupling method on a 3D numerical lattice has been applied to calculate total cross sections for the electron-impact double ionization of He [7] and H^- [8] and the

photon-impact triple ionization of Li [9], which are the simplest quantal four-body Coulomb breakup problems. The time-dependent close-coupling method on a 4D numerical lattice has also been applied to calculate total cross sections for the electron-impact single ionization of H_2^+ [10] and H_2 [11] and the photon-impact double ionization of H_2 [12], which are variants of quantal three-body Coulomb breakup problems involving a non-spherical nuclear field.

In the last decade a variety of non-perturbative theories have been developed to calculate a number of atomic and molecular collision processes with unprecedented accuracy. Several different numerical solutions of the quantal three-body Coulomb breakup problem are now routinely used to confront detailed experimental measurements. The converged close-coupling method has been reviewed for electron–helium scattering by Fursa and Bray [13] and for electron and photon collisions with atoms by Bray *et al* [14]. The *R*-matrix approach has been surveyed for a variety of atomic and molecular collision processes [15], while the inclusion of a large number of pseudo-states was first described by Bartschat *et al* [16] and Gorczyca and Badnell [17]. The exterior complex scaling method has been reviewed for electron ionization of hydrogen by McCurdy *et al* [18] and for electron–hydrogen collisions by Bartlett [19]. In this paper we present a review of time-dependent close-coupling (TDCC) theory and its application to electron and photon scattering from atoms and molecules. Unless otherwise stated, all quantities are given in atomic units.

2. Time-dependent calculations on a 2D numerical lattice

2.1. Close-coupling equations for electron scattering from atoms

The time-dependent Schrödinger equation for electron scattering from a one-electron atom is given by

$$\frac{\mathrm{i}\partial\Psi(\vec{r}_1,\vec{r}_2,t)}{\partial t} = H_{\mathrm{system}}\Psi(\vec{r}_1,\vec{r}_2,t), \tag{1}$$

where the non-relativistic Hamiltonian for the scattering system is given by

$$H_{\mathrm{system}} = \sum_{i=1}^{2}\left(-\frac{1}{2}\nabla_i^2 - \frac{Z}{r_i}\right) + \frac{1}{|\vec{r}_1-\vec{r}_2|}, \tag{2}$$

$\vec{r}_1$ and $\vec{r}_2$ are the coordinates of the two electrons, and Z is the nuclear charge. The total electronic wavefunction is expanded in coupled spherical harmonics for each total orbital angular momentum, L, and total spin angular momentum, S:

$$\Psi^{LS}(\vec{r}_1,\vec{r}_2,t) = \sum_{l_1,l_2}\frac{P^{LS}_{l_1l_2}(r_1,r_2,t)}{r_1r_2}\sum_{m_1,m_2}C^{l_1\ l_2\ L}_{m_1m_20}Y_{l_1m_1}(\hat{r_1})Y_{l_2m_2}(\hat{r_2}), \tag{3}$$

where $C^{l_1\ l_2\ l_3}_{m_1m_2m_3}$ is a Clebsch–Gordan coefficient and $Y_{lm}(\hat{r})$ is a spherical harmonic. Upon substitution of Ψ into the time-dependent Schrödinger equation, we obtain the following set of time-dependent close-coupled partial differential equations for each LS symmetry [1, 2]:

$$\mathrm{i}\frac{\partial P^{LS}_{l_1l_2}(r_1,r_2,t)}{\partial t} = T_{l_1l_2}(r_1,r_2)P^{LS}_{l_1l_2}(r_1,r_2,t) + \sum_{l_1',l_2'}V^{L}_{l_1l_2,l_1'l_2'}(r_1,r_2)P^{LS}_{l_1'l_2'}(r_1,r_2,t), \tag{4}$$

where

$$T_{l_1l_2}(r_1,r_2) = \sum_{i=1}^{2}\left(-\frac{1}{2}\frac{\partial^2}{\partial r_i^2} + \frac{l_i(l_i+1)}{2r_i^2} - \frac{Z}{r_i}\right), \tag{5}$$

and the coupling operator is given in terms of 3j and 6j symbols by

$$V^{L}_{l_1 l_2, l'_1 l'_2}(r_1, r_2) = (-1)^{l_1+l'_1+L}\sqrt{(2l_1+1)(2l'_1+1)(2l_2+1)(2l'_2+1)} \times \sum_{\lambda} \frac{(r_1, r_2)^{\lambda}_{<}}{(r_1, r_2)^{\lambda+1}_{>}} \begin{pmatrix} l_1 & \lambda & l'_1 \\ 0 & 0 & 0 \end{pmatrix} \begin{pmatrix} l_2 & \lambda & l'_2 \\ 0 & 0 & 0 \end{pmatrix} \begin{Bmatrix} l_1 & l_2 & L \\ l'_2 & l'_1 & \lambda \end{Bmatrix}. \tag{6}$$

2.2. *Close-coupling equations for photon scattering from atoms*

The time-dependent Schrödinger equation for a two electron-atom in a strong time-varying electromagnetic field is given by

$$\frac{\mathrm{i}\partial\Psi(\vec{r}_1, \vec{r}_2, t)}{\partial t} = (H_{\mathrm{atom}} + H_{\mathrm{rad}})\Psi(\vec{r}_1, \vec{r}_2, t), \tag{7}$$

where the non-relativistic Hamiltonian for the atom is given by

$$H_{\mathrm{atom}} = \sum_{i=1}^{2}\left(-\frac{1}{2}\nabla_i^2 - \frac{Z}{r_i}\right) + \frac{1}{|\vec{r}_1 - \vec{r}_2|}, \tag{8}$$

the Hamiltonian for a linearly polarized radiation field is given by

$$H_{\mathrm{rad}} = E(t)\cos\omega t \sum_{i=1}^{2} r_i \cos\theta_i, \tag{9}$$

$E(t)$ is the electric field amplitude, and ω is the radiation field frequency. Upon substitution of Ψ of equation (3) into the time-dependent Schrödinger equation of equation (7), we obtain the following set of time-dependent close-coupled partial differential equations [3]:

$$\mathrm{i}\frac{\partial P^{LS}_{l_1 l_2}(r_1, r_2, t)}{\partial t} = T_{l_1 l_2}(r_1, r_2) P^{LS}_{l_1 l_2}(r_1, r_2, t) + \sum_{l'_1, l'_2} V^{L}_{l_1 l_2, l'_1 l'_2}(r_1, r_2) P^{LS}_{l'_1 l'_2}(r_1, r_2, t) + \sum_{L'}\sum_{l'_1, l'_2} W^{LL'}_{l_1 l_2, l'_1 l'_2}(r_1, r_2, t) P^{L'S}_{l'_1 l'_2}(r_1, r_2, t), \tag{10}$$

where

$$W^{LL'}_{l_1 l_2, l'_1 l'_2}(r_1, r_2, t) = \delta_{l_2, l'_2}(-1)^{l_2}\sqrt{(2l_1+1)(2l'_1+1)(2L+1)(2L'+1)} \times r_1 E(t)\cos\omega t \begin{pmatrix} l_1 & 1 & l'_1 \\ 0 & 0 & 0 \end{pmatrix} \begin{pmatrix} L & 1 & L' \\ 0 & 0 & 0 \end{pmatrix} \begin{Bmatrix} l_1 & l_2 & L \\ L' & 1 & l'_1 \end{Bmatrix} + \delta_{l_1, l'_1}(-1)^{l_1}\sqrt{(2l_2+1)(2l'_2+1)(2L+1)(2L'+1)} \times r_2 E(t)\cos\omega t \begin{pmatrix} l_2 & 1 & l'_2 \\ 0 & 0 & 0 \end{pmatrix} \begin{pmatrix} L & 1 & L' \\ 0 & 0 & 0 \end{pmatrix} \begin{Bmatrix} l_2 & l_1 & L \\ L' & 1 & l'_2 \end{Bmatrix}. \tag{11}$$

Alternatively, the time-dependent wavefunction for a two-electron atom may be divided into two parts:

$$\Psi(\vec{r}_1, \vec{r}_2, t) = \psi_0(\vec{r}_1, \vec{r}_2)\,\mathrm{e}^{-\mathrm{i}E_0 t} + \psi(\vec{r}_1, \vec{r}_2, t), \tag{12}$$

where ψ_0 is the exact eigenfunction and E_0 is the exact eigenenergy of the time-independent atomic Hamiltonian. Substitution into the time-dependent Schrödinger equation of equation (7) yields

$$\frac{\mathrm{i}\partial\psi(\vec{r}_1, \vec{r}_2, t)}{\partial t} = (H_{\mathrm{atom}} + H_{\mathrm{rad}})\psi(\vec{r}_1, \vec{r}_2, t) + H_{\mathrm{rad}}\psi_0(\vec{r}_1, \vec{r}_2)\,\mathrm{e}^{-\mathrm{i}E_0 t}. \tag{13}$$

In the weak-field perturbative limit, one may solve the somewhat simpler time-dependent equation given by

$$\frac{\mathrm{i}\partial\psi(\vec{r}_1,\vec{r}_2,t)}{\partial t} = H_{\mathrm{atom}}\psi(\vec{r}_1,\vec{r}_2,t) + H_{\mathrm{rad}}\psi_0(\vec{r}_1,\vec{r}_2)\,\mathrm{e}^{-\mathrm{i}E_0 t}. \tag{14}$$

Upon substitution of coupled spherical harmonic expansions for both ψ and ψ_0 into equation (14), we obtain the following set of time-dependent close-coupled partial differential equations [3]:

$$\begin{aligned}\mathrm{i}\frac{\partial P^{LS}_{l_1l_2}(r_1,r_2,t)}{\partial t} &= T_{l_1l_2}(r_1,r_2)P^{LS}_{l_1l_2}(r_1,r_2,t) + \sum_{l_1',l_2'} V^{L}_{l_1l_2,l_1'l_2'}(r_1,r_2)P^{LS}_{l_1'l_2'}(r_1,r_2,t)\\ &\quad + \sum_{l_1',l_2'} W^{LL_0}_{l_1l_2,l_1'l_2'}(r_1,r_2,t)P^{L_0S}_{l_1'l_2'}(r_1,r_2)\,\mathrm{e}^{-\mathrm{i}E_0t}.\end{aligned} \tag{15}$$

2.3. Numerical solutions

We solve the time-dependent close-coupled equations using a discrete representation of the radial wavefunctions and all operators on a two-dimensional lattice. Our specific implementation on massively parallel computers is to partition both the r_1 and r_2 coordinates over the many processors. For electron scattering, both an explicit method given by

$$P^{LS}_{l_1l_2}(t+\Delta t) = -2\mathrm{i}\Delta t\,H_{\mathrm{system}}P^{LS}_{l_1l_2}(t) + P^{LS}_{l_1l_2}(t-\Delta t), \tag{16}$$

and an implicit method given by

$$\begin{aligned}P^{LS}_{l_1l_2}(t+\Delta t) &= \sum_{l_1',l_2'} \mathrm{e}^{-\mathrm{i}\frac{\Delta t}{2}V^{L}_{l_1l_2,l_1'l_2'}(r_1,r_2)}\left(1+\mathrm{i}\frac{\Delta t}{2}\bar{T}_{l_1'}(r_1)\right)^{-1}\left(1+\mathrm{i}\frac{\Delta t}{2}\bar{T}_{l_2'}(r_2)\right)^{-1}\\ &\quad\times\left(1-\mathrm{i}\frac{\Delta t}{2}\bar{T}_{l_2'}(r_2)\right)\left(1-\mathrm{i}\frac{\Delta t}{2}\bar{T}_{l_1'}(r_1)\right)\sum_{l_1'',l_2''}\mathrm{e}^{-\mathrm{i}\frac{\Delta t}{2}V^{L}_{l_1'l_2',l_1''l_2''}(r_1,r_2)}P^{LS}_{l_1''l_2''}(t),\end{aligned} \tag{17}$$

where

$$\bar{T}_l(r) = -\frac{1}{2}\frac{\partial^2}{\partial r^2} + \frac{l(l+1)}{2r^2} - \frac{Z}{r}, \tag{18}$$

have been employed to time propagate the close-coupled partial differential equations. The explicit method involves one matrix multiplication per time step. Norm conservation is exact if we adjust the time step to be less than one divided by the eigenvalue with largest absolute value of the discrete Hamiltonian operator. The implicit method may employ much larger time steps than the explicit method, but the matrix inversion steps are much slower than the matrix multiplication steps on massively parallel computers.

2.4. Initial conditions and cross sections for electron scattering from atoms

Since the Hamiltonians in the previous section do not contain explicit spin interaction operators, the spin dependence of the final cross sections is found in the initial conditions or in the extraction of scattering probabilities.

The initial condition for the solution of the TDCC equations (equation (4)) for electron scattering from a one-electron atom may be given by

$$P^{LS}_{l_1l_2}(r_1,r_2,t=0) = P_{nl}(r_1)G_{k_0l'}(r_2)\delta_{l_1,l}\delta_{l_2,l'}, \tag{19}$$

where $P_{nl}(r)$ is a bound radial wavefunction for a one-electron atom and the Gaussian wavepacket, $G_{k_0L}(r)$, has a propagation energy of $\frac{k_0^2}{2}$. Probabilities for all the many collision

processes possible are obtained by $t \to \infty$ projection onto fully antisymmetric spatial and spin wavefunctions. For electron single ionization of the hydrogen atom, the partial collision probability is given by

$$\mathcal{P}_{l_1 l_2 L, s_1 s_2 S}(t) = \sum_{k_1} \sum_{k_2} |R(12, t) + (-1)^S R(21, t)|^2, \tag{20}$$

where

$$R(ij, t) = \int_0^\infty \mathrm{d}r_1 \int_0^\infty \mathrm{d}r_2 P_{k_1 l_1}(r_i) P_{k_2 l_2}(r_j) P^{LS}_{l_1 l_2}(r_1, r_2, t). \tag{21}$$

The $P_{kl}(r)$ are continuum radial wavefunctions for the hydrogen atom, $s_1 = s_2 = \frac{1}{2}$, and $S = 0$ or $S = 1$.

For two electron systems, in which the spatial and spin dependence of the time-dependent wavefunction may be separated, the initial condition for the solution of the TDCC equations for electron scattering from a one-electron atom may also be given by

$$P^{LS}_{l_1 l_2}(r_1, r_2, t = 0) = \sqrt{\tfrac{1}{2}}(P_{nl}(r_1) G_{k_0 l'}(r_2) \delta_{l_1, l} \delta_{l_2, l'} + (-1)^S G_{k_0 l'}(r_1) P_{nl}(r_2) \delta_{l_1, l'} \delta_{l_2, l}). \tag{22}$$

Probabilities for all the many collision processes possible are obtained by $t \to \infty$ projection onto spatial product wavefunctions. For electron single ionization of the hydrogen atom, the partial collision probability is now given by

$$\mathcal{P}_{l_1 l_2 L, s_1 s_2 S}(t) = \sum_{k_1} \sum_{k_2} |R(12, t)|^2. \tag{23}$$

We note that the collision probability for electron excitation of the hydrogen atom to an nl bound state is almost identical to equation (20) or equation (23). Simply eliminate one of the sums over electron momenta and change one of the $P_{kl}(r)$ radial wavefunctions to $P_{nl}(r)$. An alternative method for calculating single ionization probabilities is to sum over all bound state excitation probabilities, including doubly excited bound states, and subtract from a total probability of 1.

By careful monitoring of the excitation and ionization probabilities a number of useful checks may be carried out on the overall convergence of the TDCC calculations. As the time of wavefunction propagation proceeds, one should observe that the collision probabilities will find their asymptotic limit. For electron ionization near threshold, equal energy outgoing electrons at small angular separation will interact strongly for large distances, which is the worst case scenario for the quantal three-body Coulomb breakup problem. Thus, both a large numerical lattice (to thousands of Bohr radii) and a long propagation time are found to be critical in obtaining collision probability convergence. Fortunately, we have not found it necessary to make the lattice boundary size anywhere near the experimental distance from interaction cell to detector. By monitoring the collision probabilities, we may also check the lattice mesh spacing (generally a small fraction of a Bohr radius) and the $l_1 l_2$ partial wave convergence for a given LS total symmetry.

Finally, the total cross section for the electron single ionization of the hydrogen atom is given by

$$\sigma_{\mathrm{sion}} = \frac{\pi}{4k_0^2} \sum_{L,S} (2L + 1)(2S + 1) \mathcal{P}^{LS}_{\mathrm{sion}}, \tag{24}$$

where $\mathcal{P}^{LS}_{\mathrm{sion}}$ is found by summing over all $l_1 l_2$ partial collision probabilities.

2.5. Initial conditions and cross sections for photon scattering from atoms

The initial condition for the solution of the TDCC equations (equation (15)) for single photon scattering from a two-electron atom is given by

$$P^{LS}_{l_1 l_2}(r_1, r_2, t = 0) = 0. \tag{25}$$

The expansion functions $P^{L_0 S}_{l_1 l_2}(r_1, r_2)$ and energy E_0 are obtained by relaxation of the time-dependent Schrödinger equation for a two-electron atom in imaginary time. For photon double ionization of the helium atom, the partial collision probability is given by

$$\mathcal{P}_{l_1 l_2 L, s_1 s_2 S}(t) = \sum_{k_1} \sum_{k_2} |R(12, t)|^2. \tag{26}$$

The total cross section for the photon double ionization of the helium atom is given by

$$\sigma_{\text{dion}} = \frac{\omega}{I} \frac{\partial \mathcal{P}^{LS}_{\text{dion}}}{\partial t}, \tag{27}$$

where I is the radiation field intensity and $\mathcal{P}^{LS}_{\text{dion}}$ is found by summing over all $l_1 l_2$ partial collision probabilities.

2.6. Approximate two-electron Hamiltonians

The time-dependent close-coupling method has been applied to calculate the total cross section for electron-impact ionization of a target electron in the outer subshells of a multi-electron atom or ion. For one active electron outside closed subshells, e.g. the 2s orbital in Li ($1s^2 2s$), the TDCC method yields cross sections from the initial doublet term for the various electron scattering processes. For other cases, such as the 2s or 2p orbital in Be ($1s^2 2s2p$), the TDCC method yields configuration-averaged cross sections for the various electron scattering processes. To handle multi-electron atomic systems, the single particle operator in the time-dependent close-coupling equations is now given by

$$T_{l_1 l_2}(r_1, r_2) = \sum_{i=1}^{2} \left[-\frac{1}{2} \frac{\partial^2}{\partial r_i^2} + V^{l_i}_{PP}(r_i) \right], \tag{28}$$

where $V^{l}_{PP}(r)$ is an l-dependent core pseudo-potential, and the subshell occupation number of the active electron now multiplies the expression for the scattering cross sections.

Our method for determining the pseudo-potentials, $V^{l}_{PP}(r)$, is best illustrated through the example of Li ($1s^2 2s$). The $1s$ orbital is first obtained by solving the Hartree–Fock equations for $Li^+(1s^2)$. The core orbital is then used to construct the radial Hamiltonian:

$$h(r) = -\frac{1}{2} \frac{\partial^2}{\partial r^2} + V^{l}_{HX}(r), \tag{29}$$

where

$$V^{l}_{HX}(r) = \frac{l(l+1)}{2r^2} - \frac{Z}{r} + V_H(r) - \frac{\alpha_l}{2} \left(\frac{24\rho}{\pi} \right)^{1/3}. \tag{30}$$

$V_H(r)$ is the direct Hartree potential and ρ is the probability density in the local exchange potential. The excited-state spectrum is then obtained for each l by diagonalizing $h(r)$ on the lattice. The parameter α_l is varied to obtain experimental energy splittings for the first few excited states. For $l = 0$, the inner node of the 2s orbital is smoothly removed and $V^{0}_{PP}(r)$ is obtained by inverting the radial Schrödinger equation with the newly constructed 2s pseudo-orbital. For $l > 0$, $V^{l}_{PP}(r) = V^{l}_{HX}(r)$. The introduction of pseudo-potentials removes

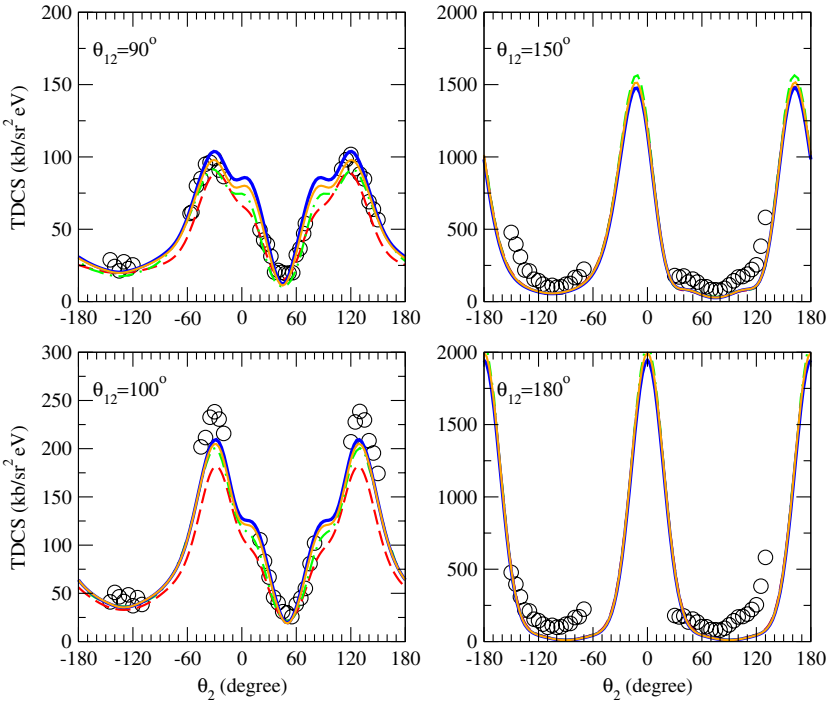

Figure 1. Electron-impact single ionization of H(1s). Solid line: time-dependent close-coupling method [25], dashed curve: converged close-coupling method [26], dot-dashed curve: exterior complex scaling method [26], open circles: experiment [26] (1 kb = 10^{-21} cm^2).

the problem of unphysical de-excitation from the active orbital to closed subshells with the same angular momentum, i.e. 2s $\rightarrow$ 1s for Li. The new radial Hamiltonian

$$h(r) = -\frac{1}{2}\frac{\partial^2}{\partial r^2} + V^0_{PP}(r), \tag{31}$$

is then diagonalized on the lattice to obtain an $l = 0$ excited pseudo-state spectrum.

2.7. Applications in electron scattering from hydrogenic atoms

One of the first applications of the time-dependent close-coupling (TDCC) method on a 2D lattice was to calculate total cross sections for electron-impact single ionization of the hydrogen atom in its ground state [1, 2]. The TDCC results were found to be in excellent agreement with converged close-coupling (CCC) [20], hyperspherical close-coupling [21], and R-matrix with pseudo-states (RMPS) [22] calculations, as well as with absolute experimental measurements [23]. The TDCC method was extended to calculate energy and angle differential cross sections for the single ionization of hydrogen in its ground state [24, 25]. For example, at an incident energy of 17.6 eV with the 4.0 eV excess energy shared equally between the outgoing electrons, the TDCC results for triple differential cross sections with the angle θ_{12} between the outgoing electrons held fixed are in excellent agreement with CCC and exterior complex scaling calculations, as well as experimental measurements [26], see figure 1.

The TDCC method was used to calculate total cross sections for electron-impact single ionization of the hydrogen atom in its 2s, 2p and 3s excited states [27, 28]. The TDCC results were found to be in excellent agreement with CCC [20] and RMPS [28] calculations,

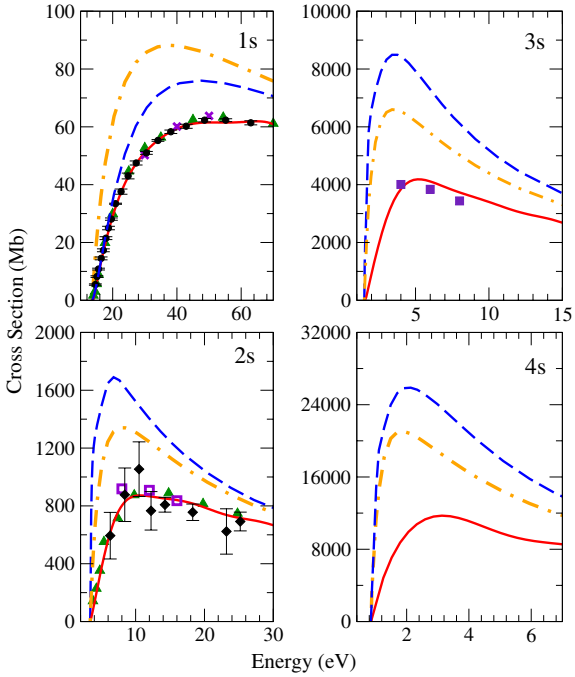

Figure 2. Electron-impact single ionization of H(ns). Crosses: time-dependent close-coupling method [2], open squares: time-dependent close-coupling method [27], solid squares: time-dependent close-coupling method [28], solid triangles: converged close-coupling method [22], solid lines: R-matrix with pseudo-states method [28], dashed and dot-dashed lines: distorted-wave method [28], solid circles: experiment [23], solid diamonds: experiment [29] (1 Mb = 10^{-18} cm^2).

and within the relatively large error bars of experimental measurements [29], see figure 2. However, the disagreement between the non-perturbative TDCC and RMPS results and the perturbative distorted-wave results increased with principal quantum number of the excited-state. With a more diffuse initial quantum state and a lower ionization potential, the quantal three-body Coulomb breakup problem becomes more difficult.

The TDCC method was used to calculate total cross sections for electron-impact single ionization of He^+ in its ground state [30] and Li^{2+} in its ground state [31] and its 2s and 4s excited states [28]. For He^+ the TDCC results were found to be in excellent agreement with CCC [32] calculations and absolute experimental measurements [33]. For Li^{2+} the TDCC results were found to be in excellent agreement with RMPS [28] calculations for the ground and excited states, and with absolute experimental measurements [34] for the ground state. The agreement between the non-perturbative TDCC and RMPS results and the perturbative distorted-wave results was found to improve for both ground and excited state ionization as one moves to higher charge states along the H isoelectronic sequence. This is in keeping with a three-body interaction that becomes dominated by a Z-dependent electron–nucleus interaction.

The TDCC method was used to calculate total cross sections for positron-impact transfer ionization of the hydrogen atom in its ground state [35]. The TDCC results were found to be in good agreement with standard close-coupling [36, 37] calculations. The partial-wave

convergence for positron–atom scattering was found to be much slower than for electron–atom scattering, due in part to the additional process of positronium formation.

2.8. Applications in electron scattering from non-hydrogenic atoms

The TDCC method with core HX potentials was used to calculate total cross sections for electron-impact single ionization of the helium atom in its $1s^2$ ground and 1s2s excited configurations [38, 39]. As well as its importance in the understanding of fundamental atomic physics, helium is an important diagnostic element in fusion plasma devices. The TDCC results for the $1s^2$ ground configuration were found to be in excellent agreement with CCC [40] and RMPS [41] calculations, as well as absolute experimental measurements [42]. On the other hand, the TDCC results for the 1s2s excited configuration were found to be in good agreement with CCC [43] calculations, but both non-perturbative results were a factor of 2 lower than experimental measurements [44]. The TDCC method was extended to calculate energy and angle differential cross sections for the single ionization of helium in its ground state [45]. We note that the TDCC method has also been used to study doubly excited states of helium and their subsequent autoionization [46].

The TDCC method with core HX potentials was used to calculate total cross sections for electron-impact single ionization of Li^+ in its $1s^2$ ground and 1s2s excited configurations [47, 48]. The TDCC results for the $1s^2$ ground configuration were found to be in very good agreement with RMPS [47] calculations and absolute experimental measurements [49–51]. The recent TDCC and RMPS [48] calculations for the 1s2s excited configuration are in excellent agreement, and thus can serve as a benchmark for future absolute experimental measurements.

The TDCC method with core HX pseudo-potentials was used to calculate total cross sections for electron-impact single ionization of the lithium atom in its $1s^22s$ ground and $1s^22p$ excited configurations [52, 53]. Lithium is also an important diagnostic element for controlled fusion, and there has been some interest in its use as a liquid metal wall in tokamaks. The TDCC results for the $1s^22s$ ground and $1s^22p$ excited configurations are in excellent agreement with CCC [53] and RMPS [53] calculations. However, all three non-perturbative calculations for the $1s^22s$ ground configuration are substantially lower than experimental measurements [54]. The TDCC method was used to calculate total cross sections for electron-impact single ionization of Be^+ in its $1s^22s$ ground configuration [55]. The TDCC results are in excellent agreement with CCC [56] and RMPS [55] calculations, but again all three non-perturbative calculations are substantially lower than experimental measurements [57]. Perturbative distorted-wave calculations [55] are found to lie almost halfway between the non-perturbative calculations and experiment. The TDCC method was used to calculate total ionization cross sections for B^{2+} in its $1s^22s$ ground configuration [58]. The TDCC results are in good agreement with CCC [59] and RMPS [58] calculations, as well as experimental measurements [58].

The TDCC method was used to calculate total cross sections for electron-impact excitation and ionization of the beryllium atom and other atomic ions in the Be isonuclear sequence [60, 61]. Recently, beryllium has been proposed as a first wall component for the plasma facing material in the planned international thermonuclear experimental reactor (ITER). The TDCC results for the $1s^22s \rightarrow 1s^22p$, $1s^23l$ and $1s^24l$ ($l = 0-2$) transitions in Be^+ are in very good agreement with CCC [56] and RMPS [60] calculations, while generally smaller than standard *R*-matrix [60] calculations for the non-dipole transitions at intermediate energies. The TDCC results for the $2s \rightarrow 3l$ and $4l$ ($l = 0-2$) transitions in Be^{3+} were also found to be in very good agreement with RMPS [60] calculations and generally smaller than standard

R-matrix [60] calculations. The TDCC results for ionization of Be in its $1s^2 2s^2$ and $1s^2 2s2p$ configurations, of Be^+ in its $1s^2 2s$ and $1s^2 2p$ configurations, and of Be^{2+} in its $1s^2$ and 1s2s configurations, were found to be in very good agreement with CCC [62, 56] and RMPS [61] calculations. The TDCC method was used to calculate total ionization cross sections for C^{2+} in its $1s^2 2s^2$ ground and $1s^2 2s2p$ excited configurations [63]. The TDCC results are in good agreement with CCC [63] and RMPS [63] calculations, while agreement with experimental measurements [63] is found when a 40%–60% mixture of ground and excited configurations is assumed in the ion beam.

The TDCC method was used to calculate total cross sections for electron-impact single ionization of the carbon atom in its $1s^2 2s^2 2p^2$ ground configuration [64], of the O^+ atomic ion in its $1s^2 2s^2 2p^3$ ground configuration [65], and of the neon atom in its $1s^2 2s^2 2p^6$ ground and $1s^2 2s^2 2p^5 3s$ excited configurations [64, 66]. For all atoms, individual LS term-selective ionization cross sections may be obtained by multiplying the configuration-average results by the appropriate branching ratio and ionization potential scaling factor. The TDCC results for the ionization of carbon in its $1s^2 2s^2 2p^2\ ^3P$ ground LS term are in good agreement with experimental measurements [67]. The TDCC results for the ionization of O^+ in its $1s^2 2s^2 2p^3$ ground configuration are also in good agreement with experimental measurements [65]. On the other hand, the TDCC results for neon in its $1s^2 2s^2 2p^6$ ground configuration are substantially above experimental measurements [68]. We attribute the disagreement between theory and experiment for neon to LS term-dependent effects in the ejected electron continuum. The TDCC results for neon in its $1s^2 2s^2 2p^5 3s$ excited configuration are in very good agreement with RMPS [66] calculations and within the error bars of experimental measurements [68], since LS term-dependent effects in the ejected electron continuum are small for the excited state ionization.

The TDCC method was used to calculate total cross sections for electron-impact single ionization of Mg^+, Al^{2+} and Si^{3+} in their $1s^2 2s^2 2p^6 3s$ ground configuration [69] and of Mo^+ in its $1s^2 2s^2 2p^6 3s^2 3p^6 3d^{10} 4s^2 4p^6 4d^5$ ground configuration [70]. The TDCC results for all three Na-like atomic ions are in good agreement with CCC [69] and RMPS [69] calculations. All three non-perturbative calculations are substantially above one set of experimental measurements [71] for Mg^+ and Al^{2+}, but are in good agreement with a more recent set of experimental measurements [72] for Mg^+. The TDCC results for Mo^+ are found to be 25% lower than perturbative distorted-wave [70] calculations, but experimental measurements [73, 74] are another 45% lower than the non-perturbative TDCC predictions. The discrepancy between theory and experiment remains unexplained.

2.9. Applications in photon scattering from atoms

One of the first applications of the time-dependent close-coupling method on a 2D lattice was to calculate total cross sections for photoionization with excitation and the double photoionization of the helium atom in its $1s^2\ ^1S$ ground state [75]. The TDCC results for $1s^2\ ^1S \rightarrow nl\ ^2l$ ($n = 2 - 3$) photoionization with excitation are in good agreement with many-body perturbation theory [76] calculations and experimental measurements [77]. The TDCC results for double photoionization are in good agreement with hyperspherical close-coupling [78], converged close-coupling [79], and *R*-matrix with pseudo-states [80, 81] calculations, as well as experimental measurements [82, 83]. Near threshold, recent large-scale TDCC results for the double photoionization of helium in its ground state [84] are in excellent agreement with experimental measurements [85] and confirm the validity of an $E^{1.056}$ power law dependency for the cross section. The TDCC method was extended to calculate energy and angle differential cross sections for the double photoionization of helium in its $1s^2\ ^1S$

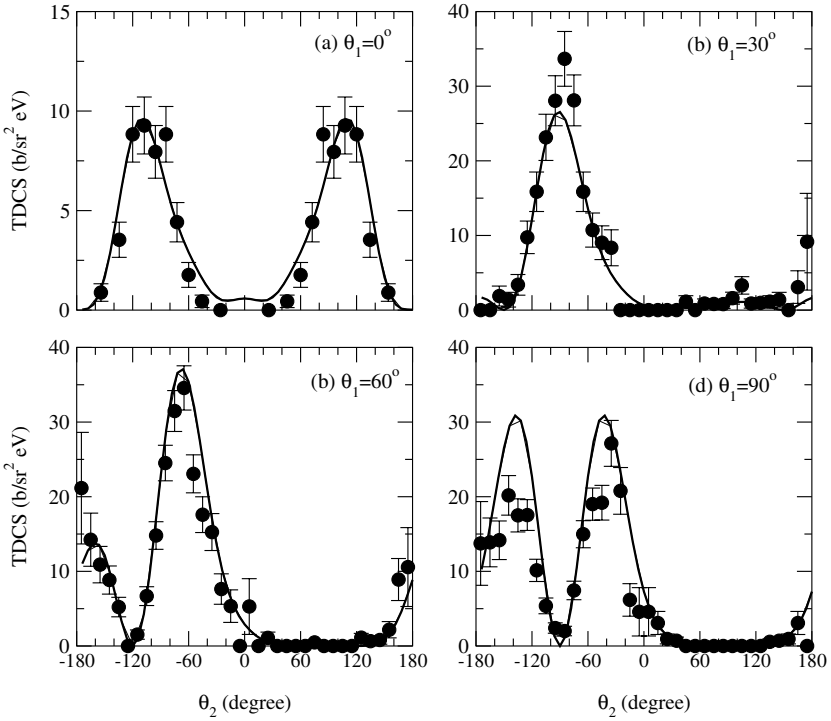

Figure 3. Photon-impact double ionization of He. Solid line: time-dependent close-coupling method [86], solid circles: experiment [90] (1 b = 10^{-24} cm^2).

ground state [86–88] and 1s2s ^{1,3}S excited states [89]. For example, with the 20.0 eV excess energy shared equally between the outgoing electrons, the TDCC results for triple differential cross sections are in excellent agreement with absolute experimental measurements [90], see figure 3.

The TDCC method was used to calculate total cross sections for photoionization with excitation and double photoionization of H^- in its $1s^2\ ^1S$ ground state [91] and Li^+ in its $1s^2\ ^1S$ ground and 1s2s ^{1,3}S excited states [92]. The TDCC results for the double photoionization of H^- are in excellent agreement with RMPS [80] calculations. The TDCC results for the photoionization with excitation and double photoionization of Li^+ in its $1s^2\ ^1S$ ground state are in good agreement with CCC [93] calculations, while the TDCC results for the double photoionization of Li^+ in its 1s2s ^{1}S excited state are somewhat higher than B-spline *R*-matrix [94] calculations. The TDCC method was recently used to calculate triple differential cross sections for the double photoionization of Li^+, Be^{2+} and B^{3+} in their ground states [95]. The TDCC method with core HX pseudo-potentials was extended to calculate total and angle differential cross sections for the double photoionization of the beryllium atom in its $1s^22s^2$ ground configuration [96].

The TDCC method was used to calculate total probabilities for two-photon double ionization processes in He and H^- [97], and then was extended to calculate energy and angle differential cross sections for the two-photon complete fragmentation of the helium atom [98]. We also note that the TDCC method has been recently used to calculate the double ionization of He by fast bare ion collisions [99]. These calculations provide theoretical

support for future experimental measurements using short wavelength free-electron lasers and heavy-ion accelerators.

3. Time-dependent calculations on a 3D numerical lattice

3.1. Close-coupling equations for electron scattering from atoms

The time-dependent Schrödinger equation for electron scattering from a two-electron atom is given by

$$\frac{\mathrm{i}\partial\Psi(\vec{r}_1,\vec{r}_2,\vec{r}_3,t)}{\partial t} = H_{\mathrm{system}}\Psi(\vec{r}_1,\vec{r}_2,\vec{r}_3,t), \tag{32}$$

where the non-relativistic Hamiltonian for the scattering system is given by

$$H_{\mathrm{system}} = \sum_{i=1}^{3}\left(-\frac{1}{2}\nabla_i^2 - \frac{Z}{r_i}\right) + \sum_{i<j=1}^{3}\frac{1}{|\vec{r}_i - \vec{r}_j|}. \tag{33}$$

The total electronic wavefunction is expanded in coupled spherical harmonics for each total orbital angular momentum, $\mathcal{L}$, and total spin angular momentum, $\mathcal{S}$:

$$\Psi^{\mathcal{LS}}(\vec{r}_1,\vec{r}_2,\vec{r}_3,t) = \sum_{l_1,l_2}\sum_{L,l_3}\frac{P^{\mathcal{LS}}_{l_1l_2Ll_3}(r_1,r_2,r_3,t)}{r_1r_2r_3} \times \sum_{M,m_3} C^{L\ l_3\ \mathcal{L}}_{Mm_30}\sum_{m_1,m_2} C^{l_1\ l_2\ L}_{m_1m_2M}Y_{l_1m_1}(\hat{r_1})Y_{l_2m_2}(\hat{r_2})Y_{l_3m_3}(\hat{r_3}). \tag{34}$$

Upon substitution of Ψ into the time-dependent Schrödinger equation, we obtain the following set of time-dependent close-coupled partial differential equations for each $\mathcal{LS}$ symmetry [7, 8]:

$$\frac{\mathrm{i}\partial P^{\mathcal{LS}}_{l_1l_2Ll_3}(r_1,r_2,r_3,t)}{\partial t} = T_{l_1l_2l_3}(r_1,r_2,r_3)P^{\mathcal{LS}}_{l_1l_2Ll_3}(r_1,r_2,r_3,t) + \sum_{l_1',l_2',L',l_3'}\sum_{i<j=1}^{3}V^{\mathcal{L}}_{l_1l_2Ll_3,l_1'l_2'L'l_3'}(r_i,r_j)P^{\mathcal{LS}}_{l_1'l_2'L'l_3'}(r_1,r_2,r_3,t), \tag{35}$$

where

$$T_{l_1l_2l_3}(r_1,r_2,r_3) = \sum_{i=1}^{3}\left(-\frac{1}{2}\frac{\partial^2}{\partial r_i^2} + \frac{l_i(l_i+1)}{2r_i^2} - \frac{Z}{r_i}\right), \tag{36}$$

and the coupling operators are given in terms of 3j and 6j symbols by

$$V^{\mathcal{L}}_{l_1l_2Ll_3,l_1'l_2'L'l_3'}(r_1,r_2) = (-1)^{l_1+l_1'+L}\delta_{l_3,l_3'}\delta_{L,L'}\sqrt{(2l_1+1)(2l_1'+1)(2l_2+1)(2l_2'+1)} \times \sum_{\lambda}\frac{(r_1,r_2)^{\lambda}_{<}}{(r_1,r_2)^{\lambda+1}_{>}}\begin{pmatrix} l_1 & \lambda & l_1' \\ 0 & 0 & 0\end{pmatrix}\begin{pmatrix} l_2 & \lambda & l_2' \\ 0 & 0 & 0\end{pmatrix}\begin{Bmatrix} l_1 & l_2 & L \\ l_2' & l_1' & \lambda\end{Bmatrix}, \tag{37}$$

$$V^{\mathcal{L}}_{l_1l_2Ll_3,l_1'l_2'L'l_3'}(r_1,r_3) = (-1)^{l_2+\mathcal{L}}\delta_{l_2,l_2'}\sqrt{(2l_1+1)(2l_1'+1)(2l_3+1)(2l_3'+1)(2L+1)(2L'+1)} \times \sum_{\lambda}(-1)^{\lambda}\frac{(r_1,r_3)^{\lambda}_{<}}{(r_1,r_3)^{\lambda+1}_{>}}\begin{pmatrix} l_1 & \lambda & l_1' \\ 0 & 0 & 0\end{pmatrix}\begin{pmatrix} l_3 & \lambda & l_3' \\ 0 & 0 & 0\end{pmatrix} \times \begin{Bmatrix} L & l_3 & \mathcal{L} \\ l_3' & L' & \lambda\end{Bmatrix}\begin{Bmatrix} l_1 & l_2 & L \\ L' & \lambda & l_1'\end{Bmatrix}, \tag{38}$$

and

$$V^{\mathcal{L}}_{l_1 l_2 L l_3, l_1' l_2' L' l_3'}(r_2, r_3) = (-1)^{l_1'+l_2+l_2'+L+L'+\mathcal{L}} \delta_{l_1, l_1'} \times \sqrt{(2l_2+1)(2l_2'+1)(2l_3+1)(2l_3'+1)(2L+1)(2L'+1)} \times \sum_{\lambda} (-1)^{\lambda} \frac{(r_2, r_3)^{\lambda}_{<}}{(r_2, r_3)^{\lambda+1}_{>}} \begin{pmatrix} l_2 & \lambda & l_2' \\ 0 & 0 & 0 \end{pmatrix} \begin{pmatrix} l_3 & \lambda & l_3' \\ 0 & 0 & 0 \end{pmatrix} \times \begin{Bmatrix} L & l_3 & \mathcal{L} \\ l_3' & L' & \lambda \end{Bmatrix} \begin{Bmatrix} l_1 & l_2 & L \\ \lambda & L' & l_2' \end{Bmatrix}. \tag{39}$$

3.2. Close-coupling equations for photon scattering from atoms

The time-dependent Schrödinger equation for a three-electron atom in a weak time-varying electromagnetic field is given by

$$\frac{\mathrm{i}\partial \psi(\vec{r}_1, \vec{r}_2, \vec{r}_3, t)}{\partial t} = H_{\mathrm{atom}} \psi(\vec{r}_1, \vec{r}_2, \vec{r}_3, t) + H_{\mathrm{rad}} \psi_0(\vec{r}_1, \vec{r}_2, \vec{r}_3)\, \mathrm{e}^{-\mathrm{i}E_0 t}, \tag{40}$$

where the non-relativistic Hamiltonian for the atom is given by

$$H_{\mathrm{atom}} = \sum_{i=1}^{3} \left(-\frac{1}{2}\nabla_i^2 - \frac{Z}{r_i} \right) + \sum_{i<j=1}^{3} \frac{1}{|\vec{r}_i - \vec{r}_j|} \tag{41}$$

and the Hamiltonian for a linearly polarized radiation field is given by

$$H_{\mathrm{rad}} = E(t) \cos \omega t \sum_{i=1}^{3} r_i \cos \theta_i. \tag{42}$$

Upon substitution of coupled spherical harmonic expansions for both ψ and ψ_0 into equation (40), we obtain the following set of time-dependent close-coupled partial differential equations [9]:

$$\frac{\mathrm{i}\partial P^{\mathcal{LS}}_{l_1 l_2 L l_3}(r_1, r_2, r_3, t)}{\partial t} = T_{l_1 l_2 l_3}(r_1, r_2, r_3) P^{\mathcal{LS}}_{l_1 l_2 L l_3}(r_1, r_2, r_3, t) + \sum_{l_1', l_2', L', l_3'} \sum_{i<j=1}^{3} V^{\mathcal{L}}_{l_1 l_2 L l_3, l_1' l_2' L' l_3'}(r_i, r_j) P^{\mathcal{LS}}_{l_1' l_2' L' l_3'}(r_1, r_2, r_3, t), + \sum_{l_1', l_2', L', l_3'} \sum_{i=1}^{3} W^{\mathcal{L}\mathcal{L}_0}_{l_1 l_2 L l_3, l_1' l_2' L' l_3'}(r_i, t) P^{\mathcal{L}_0 \mathcal{S}}_{l_1' l_2' L' l_3'}(r_1, r_2, r_3)\, \mathrm{e}^{-\mathrm{i}E_0 t}, \tag{43}$$

where

$$W^{\mathcal{L}\mathcal{L}'}_{l_1 l_2 L l_3, l_1' l_2' L' l_3'}(r_1, t) = (-1)^{l_2+l_3+L+L'+\mathcal{L}+\mathcal{L}'} \delta_{l_2, l_2'} \delta_{l_3, l_3'} \times \sqrt{(2l_1+1)(2l_1'+1)(2L+1)(2L'+1)(2\mathcal{L}+1)(2\mathcal{L}'+1)} \times r_1 E(t) \cos \omega t \begin{pmatrix} l_1 & 1 & l_1' \\ 0 & 0 & 0 \end{pmatrix} \begin{pmatrix} \mathcal{L} & 1 & \mathcal{L}' \\ 0 & 0 & 0 \end{pmatrix} \begin{Bmatrix} L & l_3 & \mathcal{L} \\ \mathcal{L}' & 1 & L' \end{Bmatrix} \begin{Bmatrix} l_1 & l_2 & L \\ L' & 1 & l_1' \end{Bmatrix}, \tag{44}$$

$$W^{\mathcal{L}\mathcal{L}'}_{l_1 l_2 L l_3, l_1' l_2' L' l_3'}(r_2, t) = (-1)^{l_1+l_2+l_2'+l_3+\mathcal{L}+\mathcal{L}'} \delta_{l_1,l_1'} \delta_{l_3,l_3'} \times \sqrt{(2l_2+1)(2l_2'+1)(2L+1)(2L'+1)(2\mathcal{L}+1)(2\mathcal{L}'+1)} \times r_2 E(t) \cos\omega t \begin{pmatrix} l_2 & 1 & l_2' \\ 0 & 0 & 0 \end{pmatrix} \begin{pmatrix} \mathcal{L} & 1 & \mathcal{L}' \\ 0 & 0 & 0 \end{pmatrix} \begin{Bmatrix} L & l_3 & \mathcal{L} \\ \mathcal{L}' & 1 & L' \end{Bmatrix} \begin{Bmatrix} l_1 & l_2 & L \\ 1 & L' & l_2' \end{Bmatrix}, \tag{45}$$

and

$$W^{\mathcal{L}\mathcal{L}'}_{l_1 l_2 L l_3, l_1' l_2' L' l_3'}(r_3, t) = (-1)^{l_3+l_3'+L+1} \delta_{l_1,l_1'} \delta_{l_2,l_2'} \delta_{L,L'} \sqrt{(2l_3+1)(2l_3'+1)(2\mathcal{L}+1)(2\mathcal{L}'+1)} \times r_3 E(t) \cos\omega t \begin{pmatrix} l_3 & 1 & l_3' \\ 0 & 0 & 0 \end{pmatrix} \begin{pmatrix} \mathcal{L} & 1 & \mathcal{L}' \\ 0 & 0 & 0 \end{pmatrix} \begin{Bmatrix} L & l_3 & \mathcal{L} \\ 1 & \mathcal{L}' & l_3' \end{Bmatrix}. \tag{46}$$

3.3. Numerical solutions

We solve the time-dependent close-coupled equations using a discrete representation of the radial wavefunctions and all operators on a three-dimensional lattice. Our specific implementation on massively parallel computers is to partition the r_1, r_2 and r_3 coordinates over the many processors. Both explicit and implicit methods have been employed to time propagate the close-coupled partial differential equations.

3.4. Initial conditions and cross sections for electron scattering from atoms

The initial condition for the solution of the TDCC equations (equation (35)) for electron scattering from a two-electron atom may be given by

$$P^{\mathcal{L}}_{l_1 l_2 L l_3}(r_1, r_2, r_3, t=0) = \sum_{l_1', l_2'} \bar{P}^{L'}_{l_1' l_2'}(r_1, r_2) G_{k_0 l_3'}(r_3) \delta_{l_1,l_1'} \delta_{l_2,l_2'} \delta_{l_3,l_3'} \delta_{L,L'}, \tag{47}$$

where $\bar{P}^{L'}_{l_1' l_2'}(r_1, r_2)$ with $L'=0$ and $l_1'=l_2'=l$ are the ground-state radial wavefunctions for the two-electron atom, obtained by relaxation of the two-electron TDCC equations in imaginary time. Probabilities for all the many collision processes are obtained by $t \to \infty$ projection onto fully antisymmetric spatial and spin wavefunctions. As an example, for electron double ionization of the ground state of the helium atom, the partial collision probability is given by

$$\begin{aligned} \mathcal{P}_{l_1 l_2 L l_3 \mathcal{L}, s_1 s_2 S s_3 \mathcal{S}}(t) = \sum_{k_1}\sum_{k_2}\sum_{k_3} \Bigg| & \sum_{L'} \delta_{L,L'} Q_a R(123,t) \\ & - \sum_{L'} (-1)^{l_2+l_3+L+L'} \sqrt{(2L+1)(2L'+1)} \begin{Bmatrix} l_2 & l_1 & L \\ l_3 & \mathcal{L} & L' \end{Bmatrix} Q_b R(132,t) \\ & - \sum_{L'} (-1)^{l_1+l_2-L'} \delta_{L,L'} Q_c R(213,t) \\ & + \sum_{L'} (-1)^{l_1+l_2+L} \sqrt{(2L+1)(2L'+1)} \begin{Bmatrix} l_2 & l_1 & L \\ l_3 & \mathcal{L} & L' \end{Bmatrix} Q_c R(312,t) \\ & + \sum_{L'} (-1)^{l_2+l_3+L'} \sqrt{(2L+1)(2L'+1)} \begin{Bmatrix} l_1 & l_2 & L \\ l_3 & \mathcal{L} & L' \end{Bmatrix} Q_b R(231,t) \\ & - \sum_{L'} \sqrt{(2L+1)(2L'+1)} \begin{Bmatrix} l_1 & l_2 & L \\ l_3 & \mathcal{L} & L' \end{Bmatrix} Q_a R(321,t) \Bigg|^2, \end{aligned} \tag{48}$$

where

$$R(ijk,t) = \int_0^\infty \mathrm{d}r_1 \int_0^\infty \mathrm{d}r_2 \int_0^\infty \mathrm{d}r_3 P_{k_1 l_1}(r_i) P_{k_2 l_2}(r_j) P_{k_3 l_3}(r_k) P^{\mathcal{L}}_{l_1 l_2 L' l_3}(r_1, r_2, r_3, t). \tag{49}$$

The $P_{kl}(r)$ are continuum radial wavefunctions for the He^+ atomic ion, $s_1 = s_2 = s_3 = \frac{1}{2}$, $Q_a = \sqrt{\frac{1}{2}}\delta_{S,0} - \sqrt{\frac{1}{6}}\delta_{S,1}$, $Q_b = \sqrt{\frac{2}{3}}\delta_{S,1}$, $Q_c = -\sqrt{\frac{1}{2}}\delta_{S,0} - \sqrt{\frac{1}{6}}\delta_{S,1}$ and $\mathcal{S} = \frac{1}{2}$.

To guard against the unwanted contribution to the partial collision probability coming from the continuum correlation part of the two-electron bound wavefunctions, one may project out the two-electron bound states from the three-electron time-propagated radial wavefunction and then project onto all electron momenta k_i. Alternatively, we found that a simple restriction of the sums over the electron momenta k_i, so that the conservation of energy,

$$E_{\mathrm{atom}} + \frac{k_0^2}{2} = \frac{k_1^2}{2} + \frac{k_2^2}{2} + \frac{k_3^2}{2}, \tag{50}$$

was approximately conserved, greatly reduced contamination from the continuum piece of the two-electron bound wavefunctions. In addition, this method of restricted momenta sums should become more accurate as the lattice size increases. We note that the collision probability for electron single ionization of the ^1S ground state of helium leaving the He^+ ion in an nl bound state is almost identical to equation (48). Simply eliminate one of the sums over electron momenta, change one of the $P_{kl}(r)$ radial wavefunctions to $P_{nl}(r)$, calculate the remaining two continuum radial wavefunctions in a $V(r)$ potential that screens the Coulomb field, and apply the relevant equation for the conservation of energy.

The total cross section for electron double ionization of the helium atom is given by

$$\sigma_{\mathrm{dion}} = \frac{\pi}{2k_0^2} \sum_{\mathcal{L},\mathcal{S}} (2\mathcal{L}+1)(2\mathcal{S}+1) \mathcal{P}^{\mathcal{L}\mathcal{S}}_{\mathrm{dion}}, \tag{51}$$

where $\mathcal{P}^{\mathcal{L}\mathcal{S}}_{\mathrm{dion}}$ is found by summing over all $l_1 l_2 L l_3$ partial collision probabilities.

3.5. Initial conditions and cross sections for photon scattering from atoms

The initial condition for the solution of the TDCC equations (equation (43)) for single photon scattering from a three-electron atom is given by

$$P^{\mathcal{L}\mathcal{S}}_{l_1 l_2 L l_3}(r_1, r_2, r_3, t = 0) = 0. \tag{52}$$

The expansion functions $P^{\mathcal{L}_0\mathcal{S}}_{l_1 l_2 L l_3}(r_1, r_2, r_3)$ and energy E_0 are obtained by relaxation of the time-dependent Schrödinger equation for a three-electron atom in imaginary time. Probabilities for all the many collision processes are again obtained by $t \to \infty$ projection onto fully antisymmetric spatial and spin wavefunctions. The total cross section for photon triple ionization of the lithium atom is given by

$$\sigma_{\mathrm{tion}} = \frac{\omega}{I} \frac{\partial \mathcal{P}^{\mathcal{L}\mathcal{S}}_{\mathrm{tion}}}{\partial t}, \tag{53}$$

where $\mathcal{P}^{\mathcal{L}\mathcal{S}}_{\mathrm{tion}}$ is found by summing over all $l_1 l_2 L l_3$ partial collision probabilities.

3.6. Applications in electron scattering from atoms

One of the first applications of the time-dependent close-coupling method on a 3D lattice was to calculate total cross sections for electron-impact single and double ionization of the helium atom in its ground state [7]. The TDCC results for single ionization, leaving He^+ in the 1s ground state, are in excellent agreement with previous TDCC with core HX potentials [38] calculations and experimental measurements [42]. The TDCC results for single ionization,

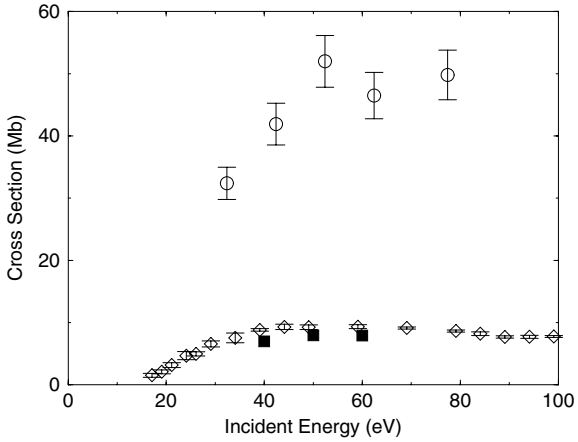

Figure 4. Electron-impact double ionization of H^-. Solid squares: time-dependent close-coupling method [8], open circles: crossed-beams experiment [104], open diamonds: crossed-beams experiment [105] (1 Mb = 10^{-18} cm^2).

leaving He^+ in the 2p excited state, are halfway between hybrid distorted-wave/R-matrix [100] calculations and experimental measurements [101, 102]. The TDCC results for double ionization are in excellent agreement with experimental measurements [103] from threshold to just below the peak of the cross section.

The TDCC method was used to calculate total cross sections for electron-impact double ionization of H^- in its ground state [8]. The TDCC results are a factor of 5 below one set of experimental measurements [104], but in very good agreement with a more recent set of experimental measurements [105], see figure 4. We note that the TDCC method has also been used to study triply excited states of He^- and Li and their subsequent single and double autoionization [106, 107].

3.7. Applications in photon scattering from atoms

One of the first applications of the time-dependent close-coupling method on a 3D lattice was to calculate total cross sections for the double and triple photoionization of the lithium atom in its $1s^2 2s\,^2S$ ground state [9, 108]. The TDCC results for double photoionization are in excellent agreement with experimental measurements [109], while the TDCC results for triple photoionization are in reasonable agreement with experimental measurements [110]. The TDCC with core HX potentials method was also used to calculate double and triple photoionization cross sections for the beryllium atom [108]. The TDCC method was extended to calculate energy differential cross sections for the triple photoionization of the lithium atom [111]. The energy differential cross section is generally below 10^{-3} barns $(eV)^{-2}$ and will be a challenge to measure for future advanced light source experiments.

4. Time-dependent calculations on a 4D numerical lattice

4.1. Close-coupling equations for electron scattering from molecules

The time-dependent Schrödinger equation for electron scattering from a one-electron homonuclear diatomic molecule is given by

$$\frac{\mathrm{i}\partial\Psi(\vec{r}_1,\vec{r}_2,t)}{\partial t} = H_{\mathrm{system}}\Psi(\vec{r}_1,\vec{r}_2,t), \tag{54}$$

where the non-relativistic Hamiltonian for the scattering system is given by

$$H_{\mathrm{system}} = \sum_{i=1}^{2}\left(-\frac{1}{2}\nabla_i^2 - \sum_{\pm}\frac{Z}{\sqrt{r_i^2+\frac{1}{4}R^2 \pm r_i R\cos\theta_i}}\right) + \frac{1}{|\vec{r}_1-\vec{r}_2|}, \tag{55}$$

R is the internuclear distance, and Z is the charge on each nucleus. The total electronic wavefunction is expanded in rotational functions for each total angular momentum projection about the internuclear axis, M, and total spin angular momentum, S:

$$\Psi^{MS}(\vec{r}_1,\vec{r}_2,t) = \sum_{m_1,m_2}\frac{P^{MS}_{m_1m_2}(r_1,\theta_1,r_2,\theta_2,t)}{r_1r_2\sqrt{\sin\theta_1}\sqrt{\sin\theta_2}}\Phi_{m_1}(\phi_1)\Phi_{m_2}(\phi_2), \tag{56}$$

where $\Phi_m(\phi) = \frac{\mathrm{e}^{\mathrm{i}m\phi}}{\sqrt{2\pi}}$ and $M = m_1 + m_2$. Upon substitution of Ψ into the time-dependent Schrödinger equation, we obtain the following set of time-dependent close-coupled partial differential equations for each MS symmetry [10, 11]:

$$\begin{aligned}\frac{\mathrm{i}\partial P^{MS}_{m_1m_2}(r_1,\theta_1,r_2,\theta_2,t)}{\partial t} &= T_{m_1m_2}(r_1,\theta_1,r_2,\theta_2)P^{MS}_{m_1m_2}(r_1,\theta_1,r_2,\theta_2,t)\\ &\times\sum_{m_1',m_2'}V^{M}_{m_1m_2,m_1'm_2'}(r_1,\theta_1,r_2,\theta_2)P^{MS}_{m_1'm_2'}(r_1,\theta_1,r_2,\theta_2,t),\end{aligned} \tag{57}$$

where

$$T_{m_1m_2}(r_1,\theta_1,r_2,\theta_2) = \sum_{i=1}^{2}\left(K(r_i)+K(r_i,\theta_i)+\frac{m_i^2}{2r_i^2\sin^2\theta_i} - \sum_{\pm}\frac{Z}{\sqrt{r_i^2+\frac{1}{4}R^2\pm r_iR\cos\theta_i}}\right), \tag{58}$$

and K are kinetic energy operators. The coupling operator is given by

$$\begin{aligned}V^{M}_{m_1m_2,m_1'm_2'}(r_1,\theta_1,r_2,\theta_2) &= \sum_{\lambda}\frac{(r_1,r_2)^{\lambda}_{<}}{(r_1,r_2)^{\lambda+1}_{>}}\sum_{q}\frac{(\lambda-|q|)!}{(\lambda+|q|)!}P_{\lambda}^{|q|}(\cos\theta_1)P_{\lambda}^{|q|}(\cos\theta_2)\\ &\times\int_0^{2\pi}\mathrm{d}\phi_1\int_0^{2\pi}\mathrm{d}\phi_2\Phi_{m_1}(\phi_1)\Phi_{m_2}(\phi_2)\,\mathrm{e}^{\mathrm{i}q(\phi_2-\phi_1)}\Phi_{m_1'}(\phi_1)\Phi_{m_2'}(\phi_2),\end{aligned} \tag{59}$$

where $P_{\lambda}^{|q|}(\cos\theta)$ is an associated Legendre function.

4.2. Close-coupling equations for photon scattering from molecules

The time-dependent Schrödinger equation for a two-electron homonuclear diatomic molecule in a weak time-varying electromagnetic field is given by

$$\mathrm{i}\frac{\partial\psi(\vec{r}_1,\vec{r}_2,t)}{\partial t} = H_{\mathrm{mol}}\psi(\vec{r}_1,\vec{r}_2,t) + H_{\mathrm{rad}}\psi_0(\vec{r}_1,\vec{r}_2)\,\mathrm{e}^{-\mathrm{i}E_0t}, \tag{60}$$

where the non-relativistic Hamiltonian for the molecule is given by

$$H_{\mathrm{mol}} = \sum_{i=1}^{2}\left(-\frac{1}{2}\nabla_i^2 - \sum_{\pm}\frac{Z}{\sqrt{r_i^2+\frac{1}{4}R^2\pm r_iR\cos\theta_i}}\right) + \frac{1}{|\vec{r}_1-\vec{r}_2|}. \tag{61}$$

The radiation field Hamiltonian, for linear polarization with respect to the internuclear axis, is given by

$$H_{\rm rad} = E(t)\cos\omega t \sum_{i=1}^{2} r_i \cos\theta_i, \tag{62}$$

while, for circular polarization with respect to the internuclear axis, is given by

$$H_{\rm rad} = \frac{E(t)}{\sqrt{2}}\cos\omega t \sum_{i=1}^{2} r_i \sin\theta_i \, {\rm e}^{{\rm i}\phi_i}. \tag{63}$$

Upon substitution of rotational function expansions for both ψ and ψ_0 into equation (60), we obtain the following set of time-dependent close-coupled partial differential equations [12]:

$$\begin{aligned} {\rm i}\frac{\partial P^{MS}_{m_1m_2}(r_1,\theta_1,r_2,\theta_2,t)}{\partial t} &= T_{m_1m_2}(r_1,\theta_1,r_2,\theta_2)P^{MS}_{m_1m_2}(r_1,\theta_1,r_2,\theta_2,t) \\ &+ \sum_{m_1',m_2'} V^{M}_{m_1m_2,m_1'm_2'}(r_1,\theta_1,r_2,\theta_2)P^{MS}_{m_1'm_2'}(r_1,\theta_1,r_2,\theta_2,t) \\ &+ \sum_{m_1',m_2'} W^{MM_0}_{m_1m_2,m_1'm_2'}(r_1,\theta_1,r_2,\theta_2,t)P^{M_0S}_{m_1'm_2'}(r_1,\theta_1,r_2,\theta_2)\,{\rm e}^{-{\rm i}E_0t}, \end{aligned} \tag{64}$$

where, for linear polarization:

$$W^{MM'}_{m_1m_2,m_1'm_2'}(r_1,\theta_1,r_2,\theta_2,t) = E(t)\cos\omega t \sum_{i=1}^{2} r_i\cos\theta_i\delta_{m_i,m_i'}, \tag{65}$$

while, for circular polarization:

$$W^{MM'}_{m_1m_2,m_1'm_2'}(r_1,\theta_1,r_2,\theta_2,t) = \frac{E(t)}{\sqrt{2}}\cos\omega t \sum_{i=1}^{2} r_i\sin\theta_i \int_0^{2\pi} {\rm d}\phi_i\,\Phi_{m_i}(\phi_i)\,{\rm e}^{{\rm i}\phi_i}\,\Phi_{m_i'}(\phi_i). \tag{66}$$

4.3. Numerical solutions

We solve the time-dependent close-coupled equations using a discrete representation of the radial and angular wavefunctions and all operators on a four-dimensional lattice. Our specific implementation on massively parallel computers is to partition both the r_1 and r_2 coordinates over the many processors. Both explicit and implicit methods have been employed to time propagate the close-coupled partial differential equations.

4.4. Initial conditions and cross sections for electron scattering from molecules

The initial condition for the solution of the TDCC equations (equation (57)) for electron scattering from a one-electron homonuclear diatomic molecule may be given by

$$P^{MS}_{m_1m_2}(r_1,\theta_1,r_2,\theta_2,t=0) = P_{nlm}(r_1,\theta_1)G_{k_0l'm'}(r_2,\theta_2)\delta_{m_1,m}\delta_{m_2,m'}, \tag{67}$$

where $P_{nlm}(r,\theta)$ is a bound radial and angular wavefunction for a one-electron molecule. Probabilities for all the many collision processes possible are obtained by $t\to\infty$ projection onto fully antisymmetric spatial and spin wavefunctions. The total cross section for the electron single ionization of the H_2^+ molecule is given by

$$\sigma_{\rm sion} = \frac{\pi}{4k_0^2}\sum_{MSl'}(2S+1)\mathcal{P}^{MS}_{\rm sion}, \tag{68}$$

where $\mathcal{P}^{MS}_{\rm sion}$ is found by summing over all m_1m_2 partial collision probabilities.

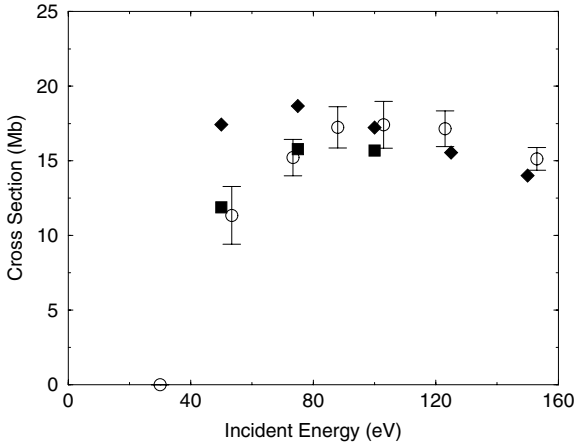

Figure 5. Electron-impact single ionization of H_2^+. Solid squares: time-dependent close-coupling method [10], solid diamonds: distorted-wave method [10], open circles: crossed-beams experiment [112] (1 Mb = 10^{-18} cm^2).

4.5. Initial conditions and cross sections for photon scattering from molecules

The initial condition for the solution of the TDCC equations (equation (64)) for single photon scattering from a two-electron homonuclear diatomic molecule is given by

$$P^{MS}_{m_1 m_2}(r_1, \theta_1, r_2, \theta_2, t = 0) = 0. \tag{69}$$

The expansion functions $P^{M_0 S}_{m_1 m_2}(r_1, \theta_1, r_2, \theta_2)$ and energy E_0 are obtained by relaxation of the time-dependent Schrödinger equation for a two-electron molecule in imaginary time. Probabilities for all the many collision processes possible are again obtained by $t \to \infty$ projection onto fully antisymmetric spatial and spin wavefunctions. The total cross section for the photon double ionization of the hydrogen molecule is given by

$$\sigma_{\text{dion}} = \frac{\omega}{I} \frac{\partial \mathcal{P}^{MS}_{\text{dion}}}{\partial t}, \tag{70}$$

where $\mathcal{P}^{MS}_{\text{dion}}$ is found by summing over all $m_1 m_2$ partial collision probabilities.

4.6. Applications in electron scattering from molecules

One of the first applications of the TDCC method on a 4D lattice was to calculate total cross sections for electron-impact single ionization of the H_2^+ molecular ion [10]. The TDCC results for single ionization are lower than perturbative distorted-wave [10] calculations and in excellent agreement with experimental measurements [112], see figure 5.

The TDCC method with core HX potentials was used to calculate total cross sections for electron-impact single ionization of the H_2 molecule [11]. The TDCC results for single ionization are in very good agreement with RMPS [113] calculations near threshold. The TDCC results from threshold to twice the peak cross section energy are lower than perturbative distorted-wave [11] calculations and in excellent agreement with experimental measurements [114].

4.7. Applications in photon scattering from molecules

One of the first applications of the TDCC method on a 4D lattice was to calculate total cross sections for the double photoionization of the H_2 molecule [12]. The TDCC results for double photoionization are in good agreement with exterior complex scaling [115] calculations and experimental measurements [116, 117]. The TDCC method was extended to calculate energy and angle differential cross sections for the double photoionization of H_2 [118].

5. Summary

The time-dependent close-coupling method has been developed and successfully applied to a wide variety of electron and photon collisions with atoms and molecules. The agreement with scattering results obtained using converged close-coupling, hyperspherical close-coupling, *R*-matrix with pseudo-states, and exterior complex scaling methods has generally been excellent. The non-perturbative methods have been successfully used to map out the range of accuracy of the more widely used perturbative quantal and semi-classical methods for a number of collision processes. The non-perturbative methods have also been used to benchmark experimental measurements, and in some cases to help decide between conflicting experimental findings. In the future we plan to continue the development of the time-dependent close-coupling method for application to a variety of atomic and molecular collision phenomena.

Acknowledgments

Over the years it has been a pleasure to collaborate with a number of distinguished scientists working on non-perturbative methods in atomic and molecular collision physics, including C Bottcher of ORNL, I Bray of Murdoch University, K Bartschat of Drake University, and C W McCurdy of LBNL. Research grant support was provided by the US Department of Energy and the US National Science Foundation. Computational support was provided by the National Energy Research Scientific Computing Center in Oakland, California and the National Center for Computational Sciences in Oak Ridge, Tennessee.

References

[1] Pindzola M S and Schultz D R 1996 *Phys. Rev.* A **53** 1525
[2] Pindzola M S and Robicheaux F 1996 *Phys. Rev.* A **54** 2142
[3] Pindzola M S and Robicheaux F 1998 *Phys. Rev.* A **57** 318
[4] Bottcher C 1985 *Adv. At. Mol. Phys.* **20** 241
[5] Wang Y D and Callaway J 1993 *Phys. Rev.* A **48** 2058
[6] Wang Y D and Callaway J 1994 *Phys. Rev.* A **50** 2327
[7] Pindzola M S, Robicheaux F, Colgan J, Witthoeft M C and Ludlow J A 2004 *Phys. Rev.* A **70** 032705
[8] Pindzola M S, Robicheaux F and Colgan J 2006 *J. Phys. B: At. Mol. Opt. Phys.* **39** L127
[9] Colgan J, Pindzola M S and Robicheaux F 2004 *Phys. Rev. Lett.* **93** 053201
[10] Pindzola M S, Robicheaux F and Colgan J 2005 *J. Phys. B: At. Mol. Opt. Phys.* **38** L285
[11] Pindzola M S, Robicheaux F, Loch S D and Colgan J 2006 *Phys. Rev.* A **73** 052706
[12] Colgan J, Pindzola M S and Robicheaux F 2004 *J. Phys. B: At. Mol. Opt. Phys.* **37** L377
[13] Fursa D V and Bray I 1997 *J. Phys. B: At. Mol. Opt. Phys.* **30** 757
[14] Bray I, Fursa D V, Kheifets A S and Stelbovics A T 2002 *J. Phys. B: At. Mol. Opt. Phys.* **35** R117
[15] Burke P G and Berrington K A (ed) 1993 *Atomic and Molecular Processes: an R-matrix Approach* (Bristol: Institute of Physics Publishing)
[16] Bartschat K, Hudson E T, Scott M P, Burke P G and Burke V M 1996 *J. Phys. B: At. Mol. Opt. Phys.* **29** 115

[17] Gorczyca T W and Badnell N R 1997 *J. Phys. B: At. Mol. Opt. Phys.* **30** 3897
[18] McCurdy C W, Baertschy M and Rescigno T N 2004 *J. Phys. B: At. Mol. Opt. Phys.* **37** R137
[19] Bartlett P L 2006 *J. Phys. B: At. Mol. Opt. Phys.* **39** R379
[20] Bray I and Stelbovics A T 1993 *Phys. Rev. Lett.* **70** 746
[21] Kato D and Watanabe S 1995 *Phys. Rev. Lett.* **74** 2443
[22] Bartschat K and Bray I 1996 *J. Phys. B: At. Mol. Opt. Phys.* **29** L577
[23] Shah M B, Elliott D S and Gilbody H B 1987 *J. Phys. B: At. Mol. Phys.* **20** 3501
[24] Colgan J, Pindzola M S, Robicheaux F, Griffin D C and Baertschy M 2002 *Phys. Rev.* A **65** 042721
[25] Colgan J and Pindzola M S 2006 *Phys. Rev.* A **74** 012713
[26] Röder J, Baertschy M and Bray I 2003 *Phys. Rev.* A **67** 010702
[27] Witthoeft M C, Loch S D and Pindzola M S 2004 *Phys. Rev.* A **70** 022711
[28] Griffin D C, Ballance C P, Pindzola M S, Robicheaux F, Loch S D, Ludlow J A, Witthoeft M C, Colgan J, Fontes C J and Schultz D R 2005 *J. Phys. B: At. Mol. Opt. Phys.* **38** L199
[29] Defrance P, Claeys W, Cornet A and Poulaert G 1981 *J. Phys. B: At. Mol. Phys.* **14** 111
[30] Witthoeft M C, Pindzola M S and Colgan J 2003 *Phys. Rev.* A **67** 032713
[31] Colgan J, Pindzola M S and Robicheaux F 2002 *Phys. Rev.* A **66** 012718
[32] Bray I, McCarthy I E, Wigley J and Stelbovics A T 1993 *J. Phys. B: At. Mol. Opt. Phys.* **26** L831
[33] Peart B, Walton D S and Dolder K T 1969 *J. Phys. B: At. Mol. Phys.* **2** 1347
[34] Tinschert K, Müller A, Hofmann G, Huber K, Becker R, Gregory D C and Salzborn E 1989 *J. Phys. B: At. Mol. Opt. Phys.* **22** 531
[35] Plante D R and Pindzola M S 1998 *Phys. Rev.* A **57** 1038
[36] Mitroy J 1996 *J. Phys. B: At. Mol. Opt. Phys.* **29** L263
[37] Kernoghan A A, Robinson D J R, McAlinden M T and Walters H R J 1996 *J. Phys. B: At. Mol. Opt. Phys.* **29** 2089
[38] Pindzola M S and Robicheaux F 2000 *Phys. Rev.* A **61** 052707
[39] Colgan J and Pindzola M S 2002 *Phys. Rev.* A **66** 062707
[40] Fursa D V and Bray I 1995 *Phys. Rev.* A **52** 1279
[41] Hudson E T, Bartschat K, Scott M P, Burke P G and Burke V M 1996 *J. Phys. B: At. Mol. Opt. Phys.* **29** 5513
[42] Montague R K, Harrison M F A and Smith A C H 1984 *J. Phys. B: At. Mol. Phys.* **17** 3295
[43] Bray I and Fursa D V 1995 *J. Phys. B: At. Mol. Opt. Phys.* **28** L197
[44] Dixon A J, Harrison M F A and Smith A C H 1976 *J. Phys. B: At. Mol. Phys.* **9** 2617
[45] Colgan J, Pindzola M S, Childers G and Khakoo M A 2006 *Phys. Rev.* A **73** 042710
[46] Mitnik D M, Griffin D C and Pindzola M S 2002 *Phys. Rev. Lett.* **88** 173004
[47] Pindzola M S, Mitnik D M, Colgan J and Griffin D C 2000 *Phys. Rev.* A **61** 052712
[48] Berengut J C, Loch S D, Ballance C P and Pindzola M S 2007 *J. Phys. B: At. Mol. Opt. Phys.* **40** 1331
[49] Lineberger W C, Hooper J W and McDaniel E W 1966 *Phys. Rev.* **141** 151
[50] Peart B and Dolder K T 1968 *J. Phys. B: At. Mol. Phys.* **2** 872
[51] Müller A, Hofmann G, Weissbecker B, Stenke M, Tinschert K, Wagner M and Salzborn E 1989 *Phys. Rev. Lett.* **63** 758
[52] Colgan J, Pindzola M S, Mitnik D M and Griffin D C 2001 *Phys. Rev.* A **63** 062709
[53] Colgan J, Pindzola M S, Mitnik D M, Griffin D C and Bray I 2001 *Phys. Rev. Lett.* **87** 213201
[54] Zapesochnyi I P and Alexsakhin I S 1969 *Sov. Phys.—JETP* **28** 41
[55] Pindzola M S, Robicheaux F, Badnell N R and Gorczyca T W 1997 *Phys. Rev.* A **56** 1994
[56] Bartschat K and Bray I 1997 *J. Phys. B: At. Mol. Opt. Phys.* **30** L109
[57] Falk R A and Dunn G H 1983 *Phys. Rev.* A **27** 754
[58] Woitke O, Djuric N, Dunn G H, Bannister M E, Smith A C H, Wallbank B, Badnell N R and Pindzola M S 1998 *Phys. Rev.* A **58** 4512
[59] Marchalant P J, Bartschat K and Bray I 1997 *J. Phys. B: At. Mol. Opt. Phys.* **30** L435
[60] Ballance C P, Griffin D C, Colgan J, Loch S D and Pindzola M S 2003 *Phys. Rev.* A **68** 062705
[61] Colgan J, Loch S D, Pindzola M S, Ballance C P and Griffin D C 2003 *Phys. Rev.* A **68** 032712
[62] Fursa D V and Bray I 1997 *J. Phys. B: At. Mol. Opt. Phys.* **30** L273
[63] Loch S D, Witthoeft M, Pindzola M S, Bray I, Fursa D V, Fogle M, Schuch R, Glans P, Ballance C P and Griffin D C 2005 *Phys. Rev.* A **71** 012716
[64] Pindzola M S, Colgan J, Robicheaux F and Griffin D C 2000 *Phys. Rev.* A **62** 042705
[65] Loch S D, Colgan J, Pindzola M S, Westermann M, Scheuermann F, Aichele K, Hathiramani D and Salzborn E 2003 *Phys. Rev.* A **67** 042714
[66] Ballance C P, Griffin D C, Ludlow J A and Pindzola M S 2004 *J. Phys. B: At. Mol. Opt. Phys.* **37** 4779
[67] Brook E, Harrison M F A and Smith A C H 1978 *J. Phys. B: At. Mol. Phys.* **11** 3115

[68] Krishnakumar E and Srivastava S K 1988 *J. Phys. B: At. Mol. Opt. Phys.* **21** 1055
[69] Badnell N R, Pindzola M S, Bray I and Griffin D C 1998 *J. Phys. B: At. Mol. Opt. Phys.* **31** 911
[70] Ludlow J A, Loch S D and Pindzola M S 2005 *Phys. Rev.* A **72** 032729
[71] Crandall D H, Phaneuf R A, Falk R A, Belic D S and Dunn G H 1982 *Phys. Rev.* A **25** 143
[72] Peart B, Thomason J W G and Dolder K 1991 *J. Phys. B: At. Mol. Opt. Phys.* **24** 4453
[73] Man K F, Smith A C H and Harrison M F A 1987 *J. Phys. B: At. Mol. Phys.* **20** 1351
[74] Hathiramani D *et al* 1996 *Phys. Rev.* A **54** 587
[75] Pindzola M S and Robicheaux F 1998 *Phys. Rev.* A **58** 779
[76] Chang T N 1980 *J. Phys. B: At. Mol. Phys.* **13** L551
[77] Wehlitz R, Sellin I A, Hemmers O, Whitfield S B, Glans P, Wang D, Lindle D W, Langer B, Berrah N, Viefhaus J and Becker U 1997 *J. Phys. B: At. Mol. Opt. Phys.* **30** L51
[78] Tang J Z and Shimamura I 1995 *Phys. Rev.* A **52** R3413
[79] Kheifets A S and Bray I 1996 *Phys. Rev.* A **54** R995
[80] Meyer K W, Greene C H and Esry B D 1997 *Phys. Rev. Lett.* **78** 4902
[81] Gorczyca T W and Badnell N R 1997 *J. Phys. B: At. Mol. Opt. Phys.* **30** 3897
[82] Levin J C, Armen G B and Sellin I A 1996 *Phys. Rev. Lett.* **76** 1220
[83] Dörner R, Vogt T, Mergel V, Khemliche H, Kravis S, Cocke C L, Ullrich J, Unverzagt M, Spielberger L, Damrau M, Jagutzki O, Ali I, Weaver B, Ullmann K, Hsu C C, Jung M, Kanter E P, Sonntag B, Prior M H, Rotenberg E, Denlinger J, Warwick T, Manson S T and Schmidt-Böcking H 1996 *Phys. Rev. Lett.* **76** 2654
[84] Kleiman U, Topcu T, Pindzola M S and Robicheaux F 2006 *J. Phys. B: At. Mol. Opt. Phys.* **39** L61
[85] Kossmann H, Schmidt V and Andersen T 1988 *Phys. Rev. Lett.* **60** 1266
[86] Colgan J, Pindzola M S and Robicheaux F 2001 *J. Phys. B: At. Mol. Opt. Phys.* **34** L457
[87] Colgan J and Pindzola M S 2002 *Phys. Rev.* A **65** 032729
[88] Colgan J and Pindzola M S 2004 *J. Phys. B: At. Mol. Opt. Phys.* **37** 1153
[89] Colgan J and Pindzola M S 2003 *Phys. Rev.* A **67** 012711
[90] Bräuning H, Dörner R, Cocke C L, Prior M H, Krassig B, Kheifets A S, Bray I, Bräuning-Demain A, Carnes K, Dreuil S, Mergel V, Richard P, Ullrich J and Schmidt-Böcking H 1998 *J. Phys. B: At. Mol. Opt. Phys.* **31** 5149
[91] Pindzola M S and Robicheaux F 1998 *Phys. Rev.* A **58** 4229
[92] Kleiman U, Pindzola M S and Robicheaux F 2005 *Phys. Rev.* A **72** 022707
[93] Kheifets A S and Bray I 1998 *Phys. Rev.* A **58** 4501
[94] van der Hart H W and Feng L 2001 *J. Phys. B: At. Mol. Opt. Phys.* **34** L247
[95] Foster M and Colgan J 2006 *J. Phys. B: At. Mol. Opt. Phys.* **39** 5067
[96] Colgan J and Pindzola M S 2002 *Phys. Rev.* A **65** 022709
[97] Pindzola M S and Robicheaux F 1998 *J. Phys. B: At. Mol. Opt. Phys.* **31** L823
[98] Colgan J and Pindzola M S 2002 *Phys. Rev. Lett.* **88** 173002
[99] Pindzola M S, Robicheaux F and Colgan J 2007 *J. Phys. B: At. Mol. Opt. Phys.* in press
[100] Raeker A, Bartschat K and Reid R H G 1994 *J. Phys. B: At. Mol. Opt. Phys.* **27** 3129
[101] Forand J L, Becker K and McConkey J W 1985 *J. Phys. B: At. Mol. Phys.* **18** 1409
[102] Hayes P A and Williams J F 1996 *Phys. Rev. Lett.* **77** 3098
[103] Shah M B, Elliott D S, McCallion P and Gilbody H P 1988 *J. Phys. B: At. Mol. Opt. Phys.* **21** 2751
[104] Peart B, Walton D S and Dolder K T 1971 *J. Phys. B: At. Mol. Phys.* **4** 88
[105] D J Yu, Rachafi S, Jureta J and Defrance P 1992 *J. Phys. B: At. Mol. Opt. Phys.* **25** 4593
[106] Pindzola M S, Robicheaux F and Colgan J 2005 *Phys. Rev.* A **72** 022709
[107] Pindzola M S, Robicheaux F and Colgan J 2006 *Phys. Rev.* A **73** 062720
[108] Colgan J, Pindzola M S and Robicheaux F 2005 *Phys. Rev.* A **72** 022727
[109] Huang M T, Wehlitz R, Azuma Y, Pibida L, Sellin I A, Cooper J W, Koide M, Ishijima H and Nagata T 1999 *Phys. Rev.* A **59** 3397
[110] Wehlitz R, Huang M T, DePaola B D, Levin J C, Sellin I A, Nagata T, Cooper J W and Azuma Y 1998 *Phys. Rev. Lett.* **81** 1813
[111] Colgan J and Pindzola M S 2006 *J. Phys. B: At. Mol. Opt. Phys.* **39** 1879
[112] Peart B and Dolder K T 1973 *J. Phys. B: At. Mol. Phys.* **6** 2409
[113] Gorfinkiel J D and Tennyson J 2005 *J. Phys. B: At. Mol. Opt. Phys.* **38** 1607
[114] Staub H C, Renault P, Lindsay B G, Smith K A and Stebbings R F 1996 *Phys. Rev.* A **54** 2146
[115] Vanroose W, Martin F, Rescigno T N and McCurdy C W 2004 *Phys. Rev.* A **70** 050703
[116] Dujardin G, Besnard M J, Hellner L and Malinovitch Y 1987 *Phys. Rev.* A **35** 5012
[117] Kossmann H, Schwarzkopf O, Kammerling B and Schmidt V 1989 *Phys. Rev. Lett.* **63** 2040
[118] Colgan J, Pindzola M S and Robicheaux F 2007 *Phys. Rev. Lett.* in press